The Journal of Chemical Physics

Compressed representation of dispersion interactions and long-range electronic correlations

Cite as: J. Chem. Phys. **147**, 144110 (2017); https://doi.org/10.1063/1.4997186
Submitted: 21 July 2017 • Accepted: 27 September 2017 • Published Online: 13 October 2017

Jérôme F. Gonthier and Martin Head-Gordon

Compressed representation of dispersion interactions and long-range electronic correlations

Jérôme F. Gonthier[a)] and Martin Head-Gordon[b)]
Kenneth S. Pitzer Center for Theoretical Chemistry, Department of Chemistry, University of California, Berkeley, California 94720, USA and Chemical Sciences Division, Lawrence Berkeley National Laboratory, Berkeley, California 94720, USA

(Received 21 July 2017; accepted 27 September 2017; published online 13 October 2017)

The description of electron correlation in quantum chemistry often relies on multi-index quantities. Here, we examine a compressed representation of the long-range part of electron correlation that is associated with dispersion interactions. For this purpose, we perform coupled-cluster singles and doubles (CCSD) computations on localized orbitals, and then extract the portion of CCSD amplitudes corresponding to dispersion energies. Using singular value decomposition, we uncover that a very compressed representation of the amplitudes is possible in terms of occupied-virtual geminal pairs located on each monomer. These geminals provide an accurate description of dispersion energies at medium and long distances. The corresponding virtual orbitals are examined by further singular value decompositions of the geminals. We connect each component of the virtual space to the multipole expansion of dispersion energies. Our results are robust with respect to basis set change and hold for systems as large as the benzene-methane dimer. This compressed representation of dispersion energies paves the way to practical and accurate approximations for dispersion, for example, in local correlation methods. *Published by AIP Publishing.* https://doi.org/10.1063/1.4997186

I. INTRODUCTION

In quantum chemistry, the description of electron correlation often relies on multi-index quantities, which are tensors.[1] The four-index tensor of four-center two-electron integrals is perhaps the most familiar one. It is natural to ask whether such tensors can be efficiently approximated using sums of products of lower-rank tensors. One way to motivate that question is by the well-known result that positive semi-definite matrices can be diagonalized and approximated in a least squares sense by discarding small eigenvalues. Singular value decomposition (SVD)[2] generalizes this result to non-symmetric matrices, providing a factorization in terms of a sum of vector outer products. These vectors are ranked by an associated singular value, and selecting the N vectors with the largest singular value provides the least-squares optimal rank-N representation of the original matrix. A matrix whose effective rank is much smaller than its dimensions can be accurately approximated with only a small fraction of its eigenvalues or singular values.

Indeed, there are many successful strategies that express 4-center two-electron integrals as sums of products of two and three center integrals. These include density fitting,[3–5] resolution of the identity,[6,7] or Cholesky decomposition.[8–10] Of course, accurate quantum chemistry computations must include electronic correlation effects, which introduces further high-dimensional tensors in the theory. Well-known examples are the doubles ($\mathcal{T}_2$) and triples ($\mathcal{T}_3$) amplitudes of coupled cluster (CC) theory.[1] Can such amplitudes likewise be compressed? After a review of relevant existing work, this paper addresses that question for $\mathcal{T}_2$-type amplitudes that correspond to dispersive correlations—where two electrons undergo correlated fluctuations at spatially separated sites.

First we note that one can apply SVD to higher-order tensors directly by grouping some of their indices together to effectively form a two-dimensional matrix, a process we will refer to as unfolding. This technique was first applied to the CC $\mathcal{T}_2$ amplitudes[11] and later extended to approximate perturbative $\mathcal{T}_3$ amplitudes[12] to reduce computational cost while preserving accuracy. Such tensor decompositions allow us to gain physical insight into complex amplitudes by adaptively extracting the most relevant information. For example, the unfolding and SVD of the $\mathcal{T}_2$ amplitude tensor yields the dominant pair correlations, represented as two-electron geminal hole and particle functions.[13] A generalization of SVD[14] for high-order tensors has also been applied to the $\mathcal{T}_2$ amplitudes[15] for analysis.

There have also been efforts to use different tensor decomposition approaches tailored to evaluating the electronic correlation energy.[16,17] Other examples include the low-rank spectral expansion;[18] tensor hypercontraction,[19,20] and generalized Cholesky methods.[21] Additionally, the Density Matrix Renormalization Group (DMRG)[22,23] is an approximate full CI algorithm that expresses the high dimensional electronic wavefunction as a sum of products of lower-dimensional quantities.[24] This naturally yields a compact representation with reduced computational cost, particularly for quasi-one-dimensional problems, reflecting the underlying tensor decomposition.

[a)]j.gonthier01@gmail.com
[b)]mhg@cchem.berkeley.edu

In general, natural orbitals (NOs) are the eigenvectors that are obtained by SVD of a density matrix,[25] for which they offer a compact description. The occupation number of NOs ranks them by their importance in the description of the corresponding density matrix. Thus, obtaining NOs from a correlated density matrix at a low level of theory offers a way of truncating the virtual space in a high-level correlated computation.[26–28] NOs, often extracted from affordable MP2 computations, are also extremely useful in local correlation methods,[29,30] as exemplified by Pair Natural Orbitals (PNOs),[31,32] that tailor the virtual space to each electron pair and that are extracted from the appropriate density matrix by SVD. PNOs were recently revisited with much success for accurate local correlation methods.[33,34] Alternatively, SVD of the diagonal MP2 amplitudes yields sets of Orbital-Specific Virtuals (OSVs) for each occupied orbital,[35] a reduced representation that was also applied to coupled-cluster singles and doubles with perturbative triples correction [CCSD(T)].[36,37]

The existence of a reduced correlation space for the dispersive correlation of distant electron pairs was already mentioned by Pulay in one of his earliest papers on local correlation:[29] "*Indeed, in the van der Waals limit interpair correlation can be probably described by using only three correlation functions, corresponding to the three components of the instantaneous dipole moment.*" To our knowledge, a recent paper[38] on improved PNO methods based on iterating the distant CC amplitudes in a reduced virtual correlation space is the first to actually adopt such an approach in practice, and no detailed investigation of a compressed representation for dispersion or long-range electron correlation yet exists. This paper aims to fill this gap; we will compare our numerical results against Pulay's prediction and against the improved PNO method for long-range correlations[38] in Sec. IV C.

Our work investigates in detail a tensor decomposition of dispersion interactions, with a particular focus on the monomer virtual orbitals needed for an accurate description. Section II summarizes our method and the associated theory before presenting the two groups of dimers that will serve as our models and the necessary computational details. In Sec. III, we show that the amplitudes describing correlation between distant electron pairs can be greatly compressed. We examine first minimal monomers, and then extract the virtual orbitals characteristic of this compressed representation. We highlight the major role played by 2p and 3p orbitals in systems with a single electron pair. We extend our considerations to larger systems as well. In Sec. IV, we investigate the accuracy of our approximate amplitudes in reproducing dispersion energies, both in small and large monomers. In all cases, we obtain accurate results using a minimal number of virtual orbitals. Finally, Sec. V offers a summary of our main results and our conclusions.

II. THEORETICAL METHODS AND MODEL SYSTEMS

A. Definition of dispersion energies

Here, we will follow the widely accepted definition of dispersion energies from long-range perturbation theory.[39] When describing two monomers A and B with a Hartree-Fock wavefunction, the expression for dispersion energy reads

$$E_{disp} = \sum_{ia}^{A} \sum_{jb}^{B} \frac{(ia|jb)\,(ai|bj)}{\epsilon_a + \epsilon_b - \epsilon_i - \epsilon j}. \tag{1}$$

Here $(ia|jb)$ represents a molecular electron repulsion integral in the chemist's notation, where i and a are, respectively, occupied and virtual orbitals on monomer A, whereas j and b are occupied and virtual orbitals on monomer B. ϵ_x is the Hartree-Fock orbital energy of orbital x. The only assumption that is made in deriving this expression is that exchange interactions between monomers are negligible. Since exchange decays exponentially with distance, we expect Eq. (1) to be reasonably accurate even at medium range. Defining

$$t_{ij}^{ab} = \frac{(ia|jb)}{\epsilon_a + \epsilon_b - \epsilon_i - \epsilon j}, \tag{2}$$

we can simply rewrite the dispersion energy as

$$E_{disp} = \sum_{ia}^{A} \sum_{jb}^{B} t_{ij}^{ab}\,(ai|bj). \tag{3}$$

In the following, it will be useful to expand the $(ai|$ charge density as

$$(ai| = \sum_{\alpha} \left(\mu_\alpha^A\right)_{ai} + \sum_{\alpha\beta} \left(\Theta_{\alpha\beta}^A\right)_{ai} + \ldots \tag{4}$$

and similarly for $|bj)$, where $\left(\mu_\alpha^X\right)_{ai} = \left(a\left|\hat{\mu}_\alpha^X\right|i\right)$ and $\left(\Theta_{\alpha\beta}^X\right)_{ai} = \left(a\left|\hat{\Theta}_{\alpha\beta}^X\right|i\right)$ are matrix elements of the dipole and quadrupole operators for monomer X, respectively. The Greek letters α, β, ... index the components of each operator. Following Stone,[39] we can now write the interaction between the $(ai|$ and $|bj)$ charge densities, truncated at the quadrupole terms, as

$$(ai|bj) = D_{\mu\mu}^{aibj} + D_{\mu\Theta}^{aibj} + D_{\Theta\Theta}^{aibj} + \ldots, \tag{5}$$

where

$$D_{\mu\mu}^{aibj} = \sum_{\alpha\beta} T_{\alpha\beta} \left(\mu_\alpha^A\right)_{ai} \left(\mu_\beta^B\right)_{bj} \tag{6}$$

is the dipole-dipole term,

$$D_{\mu\Theta}^{aibj} = \sum_{\alpha\beta\gamma} T_{\alpha\beta\gamma} \left(\left(\mu_\alpha^A\right)_{ai} \left(\Theta_{\beta\gamma}^B\right)_{bj} + \left(\Theta_{\alpha\beta}^A\right)_{ai} \left(\mu_\gamma^B\right)_{bj}\right) \tag{7}$$

is the dipole-quadrupole term, and

$$D_{\Theta\Theta}^{aibj} = \sum_{\alpha\beta\gamma\delta} T_{\alpha\beta\gamma\delta} \left(\Theta_{\alpha\beta}^A\right)_{ai} \left(\Theta_{\gamma\delta}^B\right)_{bj} \tag{8}$$

is the quadrupole-quadrupole term. The T tensors contain the dependence of each interaction on the intermolecular distance R so that $T_{\alpha\beta} \propto R^{-3}$, $T_{\alpha\beta\gamma} \propto R^{-4}$, and $T_{\alpha\beta\gamma\delta} \propto R^{-5}$. We can expand both integrals in Eq. (1) to obtain

$$E_{disp} = \sum_{ia}^{A} \sum_{jb}^{B} \frac{\left(D_{\mu\mu}^{aibj}\right)^2 + \left(D_{\mu\Theta}^{aibj}\right)^2 + \left(D_{\Theta\Theta}^{aibj}\right)^2}{\epsilon_a + \epsilon_b - \epsilon_i - \epsilon_j} + 2 \sum_{ia}^{A} \sum_{jb}^{B} \frac{D_{\mu\mu}^{aibj} D_{\mu\Theta}^{aibj} + D_{\mu\Theta}^{aibj} D_{\Theta\Theta}^{aibj}}{\epsilon_a + \epsilon_b - \epsilon_i - \epsilon_j}, \tag{9}$$

where we separated terms that decay as even or odd powers of R. Thus E_{disp} is asymptotically dominated by the purely

dipolar term $\left(D^{aibj}_{\mu\mu}\right)^2$ that decays as R^{-6}. The next even-powered terms are the pure dipole-quadrupole interaction $\left(D^{aibj}_{\mu\Theta}\right)^2$ that decays as R^{-8} and the pure quadrupole-quadrupole interaction $\left(D^{aibj}_{\Theta\Theta}\right)^2$ that decays as R^{-10}. The mixed odd-powered terms $D^{aibj}_{\mu\mu}D^{aibj}_{\mu\Theta}$ and $D^{aibj}_{\mu\Theta}D^{aibj}_{\Theta\Theta}$ decay, respectively, as R^{-7} and R^{-9} and vanish for centrosymmetric molecules and atoms.

Provided we can attribute each orbital to a single monomer, Eq. (3) is easily identified from the MP2 dimer energy if exchange effects are negligible. In this case, Eq. (2) for the amplitudes is equivalent to the expression for the MP2 amplitudes. Because MP2 is known to overestimate dispersion in the basis set limit,[40,41] we replace MP2 amplitudes by CCSD amplitudes in Eq. (3). Thus, we directly identify dispersion energy from the CCSD energy expression. This identification is not new and was already employed in energy decomposition analyses, with the difference that dispersion is usually grouped with an exchange-dispersion term.[42–44] In the present work, we do not consider exchange-dispersion since we are only interested in the behavior of the interaction energy in the long range, where exchange is negligible.

Practically, we perform a Hartree-Fock computation on the dimer of interest, followed by orbital localization of the occupied and the virtual space separately using the Boys algorithm.[45–48] The orbitals are then canonicalized for each monomer separately using the monomer blocks of the dimer Fock operator. This improves considerably the convergence properties of the following CCSD computation. Upon convergence, the CCSD $\mathcal{T}_2$ doubles amplitude tensor is read, and amplitudes t^{ab}_{ij} with i and a on monomer A and j and b on monomer B are collected in a four-index dispersion amplitude tensor $\mathcal{T}_2^{disp}$. At this point, we proceed with the numerical analysis described in Sec. II B.

To obtain dispersion energies, we build the tensor $\mathcal{T}_2^{disp,sym}$ that is a symmetrized version of $\mathcal{T}_2^{disp}$ where all elements obey the following relations: $t^{ab}_{ij} = t^{ba}_{ji}$, $t^{ab}_{ij} = -t^{ba}_{ij}$, and $t^{ab}_{ij} = -t^{ab}_{ji}$. Dispersion is then computed as the difference between the CCSD energy with the full $\mathcal{T}_2$ and the CCSD energy with $\mathcal{T}_2 - \mathcal{T}_2^{disp,sym}$. Once again, we assume that the exchange component in this energy decays exponentially with monomer separation and quickly becomes negligible.

B. Tensor decomposition strategy

As mentioned in the Introduction, obtaining optimal low-dimensional decompositions for a tensor of more than two dimensions is not trivial.[49] Here, we choose to decompose the four-index $\mathcal{T}_2^{disp}$ tensor in two steps.

In the first step, we unfold the tensor, i.e., we group indices together to obtain a matrix representation of the tensor. For $\mathcal{T}_2$, there are different possible ways to group indices together. Most, if not all, of the previous work on $\mathcal{T}_2$ compression has chosen to group occupied indices together, leaving virtual indices for the second dimension of the matrix.[13,15] In the following, we denote this particular unfolding of the tensor as $\mathbf{T}^{OO,VV}$ which is a matrix with O^2 rows and V^2 columns where O and V are, respectively, the number of occupied and virtual orbitals. PNOs, for example, are computed from this unfolding by restricting the occupied indices to a single orbital pair and then performing a singular value decomposition on the resulting V^2 matrix.[32] The $\mathbf{T}^{OO,VV}$ unfolding makes a lot of sense for short-range electron correlation since it physically represents the correlation of a pair of occupied orbitals i, j into pairs of virtual orbitals a, b. In addition, the corresponding SVD yields at most O^2 significant vectors, assuming $V \leq O$.

Dispersion interactions however are most often understood in terms of correlated electron fluctuations. Expressions from long-range perturbation theory[39] connect dispersion to simultaneous electronic excitations on both monomers. To preserve this monomer-based view of dispersion, we unfold $\mathcal{T}_2^{disp}$ as $\mathbf{T}^{O_AV_A,O_BV_B}$ where O_X and V_X are the occupied and virtual orbitals of monomer X. This unfolding groups together orbitals belonging to each monomer, with O_AV_A rows and O_BV_B columns. Singular value decomposition[2] factorizes our unfolding as the product of three matrices,

$$\mathbf{T}^{O_AV_A,O_BV_B} = \mathbf{G}^A\mathbf{\Gamma}\left(\mathbf{G}^B\right)^T, \tag{10}$$

where $\mathbf{G}^A$ contains N_{gem} singular vectors which are columns of O_AV_A elements each while $\mathbf{G}^B$ contains N_{gem} singular vectors which are columns of O_BV_B elements each. $\mathbf{\Gamma}$ is a diagonal square matrix with N_{gem} singular values on the diagonal. By the properties of the SVD, N_{gem} is equal to O_AV_A if $O_AV_A \leq O_BV_B$ and to O_BV_B otherwise. Defining $\mathbf{G}^X_{\bullet P}$ as the Pth column of matrix $\mathbf{G}^X$, we can rewrite the above decomposition in terms of the singular vectors directly,

$$\mathbf{T}^{O_AV_A,O_BV_B} = \sum_P^{N_{gem}} \mathbf{G}^A_{\bullet P}\gamma_P\left(\mathbf{G}^B_{\bullet P}\right)^T. \tag{11}$$

Thus we obtain a representation of $\mathcal{T}_2^{disp}$ as a weighted sum of paired singular vectors $\mathbf{G}^A_{\bullet P}$ and $\mathbf{G}^B_{\bullet P}$, with the weight being the singular value γ_P. Since the paired singular vectors each contain both occupied and virtual orbitals, we interpret them as describing correlated electron excitations between monomers A and B. The singular values γ_P offer us a straightforward way to rank these excitations by their importance in the dispersion tensor $\mathcal{T}_2^{disp}$. In the following, for brevity and because the singular vectors represent 6-dimensional hole-particle functions, we will simply refer to them as geminals.

In the second step of our analysis, we investigate the virtual space associated with each geminal. For this purpose, we select a particular geminal P from either $\mathbf{G}^A$ or $\mathbf{G}^B$ and we unfold it as $\left(\mathbf{G}^X_{\bullet P}\right)^{O_X,V_X}$ with O_X rows and V_X columns. SVD of this matrix yields the following factorization:

$$\left(\mathbf{G}^X_{\bullet P}\right)^{O_X,V_X} = \mathbf{U}\mathbf{\Sigma}\left(\mathbf{V}\right)^T. \tag{12}$$

We assume that $O_X \leq V_X$ and thus $\mathbf{U}$ and $\mathbf{V}$ contain O_X columns that are singular vectors composed of O_X and V_X elements, respectively. $\mathbf{\Sigma}$ is a diagonal square matrix of O_X singular values σ. The columns of matrices $\mathbf{U}$ and $\mathbf{V}$ define new occupied and virtual orbitals that completely describe the chosen geminal. The occupied and virtual orbitals obtained form pairs of the so-called Natural Transition Orbitals[50,51] (NTOs). NTOs have been applied to analyze excitation amplitudes in various excited state methods like Time-Dependent Density

Functional Theory (TDDFT)[51] or Configuration Interaction Singles (CIS).[52] In our case, we analyze excitation geminals extracted from $\mathcal{T}_2^{disp}$ for which we obtain O_X pairs of occupied and virtual orbitals. We then plot the virtual orbitals using VMD[53] and GIMP (www.gimp.org). Note that if we restrict indices i and j to a single orbital pair, then each geminal corresponds to a Pair Natural Orbital (PNO),[31,32] whereas if i and j correspond to the same orbitals, we obtain Orbital-Specific Virtuals (OSVs).[35]

C. Model systems

To facilitate the interpretation of our results, we first restrict our approach to monomers that only have one occupied orbital. Our three initial dimers are thus the He dimer, H_2 in the singlet ground state, and H_2 at the triplet ground state, all computed at varying interatomic distances. To investigate the influence of a multi-atomic monomer, we analyzed He interacting with H_2 where the interfragment distance is measured between He and the H_2 center of mass, the H–H axis is perpendicular to the interfragment axis, and the H–H distance is 0.74 Å. Finally, as a first glimpse into the many-orbital monomer regime, we studied He interacting with Be. Most computations on these systems were performed with the d-aug-cc-pVQZ basis set[54–56] except where mentioned otherwise.

Then, we validated and extended our analysis on polyatomic systems, including the Ne dimer, the methane dimer, the ethene dimer, the ethene-ethyne dimer, and the methane-benzene dimer. The geometries of the methane dimer and the methane-benzene dimer were obtained from the S22 database of noncovalent complexes,[40] whereas the A24[57] data set provided geometries for ethene-ethyne and ethene dimer. We selected the parallel π-stacked geometry of the ethene dimer (number 23 in the dataset) as a model for π-stacking aromatic interactions. In all cases, the geometries from the different datasets were obtained from the online BEGDB database[58] (www.begdb.com).

The Ne dimer was investigated at separations of 3.0, 6.0, and 9.0 Å using the aug-cc-pVQZ basis set. All the other large complexes were examined with the aug-cc-pVTZ basis set at the geometries provided in the respective dataset and at distances elongated by 3.0 and 6.0 Å along the axis linking the monomers' centers of mass. When interfragment distances are reported, they correspond to the C···C distance for the methane dimer, to the distance between the two molecular planes for the ethene dimer and ethene-ethyne dimer, and to the distance between the benzene plane and the closest methane H for the benzene-methane dimer. All our computations were done at the CCSD level in Q-Chem version 4.4.[59]

III. COMPRESSIBILITY OF $\mathcal{T}_2^{disp}$

A. Small monomers

The first question that we wish to address in this work is whether there exists a compressed representation for the dispersion amplitudes. We performed a singular value decomposition of the $\mathcal{T}_2^{disp}$ tensor for CCSD computations on the He dimer at 3.0, 6.0, and 9.0 Å interatomic separation. To assess the basis set dependence of our results, the obtained singular

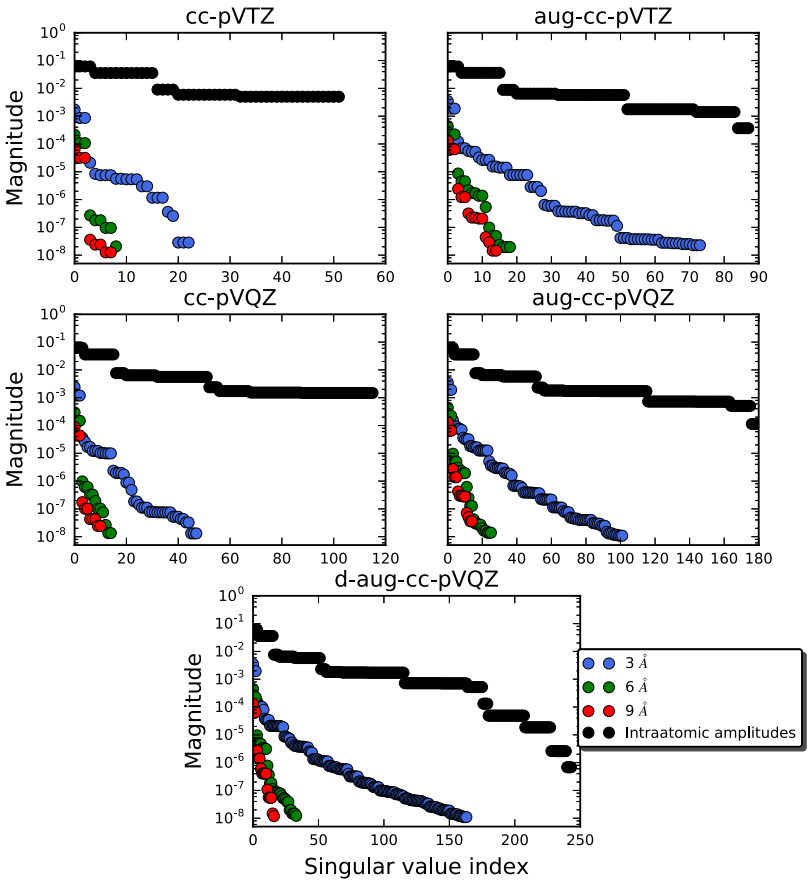

FIG. 1. $\mathcal{T}_2^{disp}$ singular values for He_2 at 3.0 Å (blue), 6.0 Å (green), and 9.0 Å (red) interatomic separation with the cc-pVTZ, cc-pVQZ, aug-cc-pVTZ, aug-cc-pVQZ, and d-aug-cc-pVQZ basis sets. In black, we plot the singular values for intraatomic amplitudes in He. The basis set used is indicated above each plot.

values γ_P are plotted in Fig. 1 for the cc-pVTZ, cc-pVQZ, aug-cc-pVTZ, aug-cc-pVQZ, and d-aug-cc-pVQZ basis sets. We also plotted for comparison the singular values obtained when decomposing the intraatomic $\mathcal{T}_2^{intra}$ amplitude tensor with the same unfolding, which represents the effect of short-range electron correlation (in black in Fig. 1).

As expected, we observe that the singular values associated with $\mathcal{T}_2^{intra}$ decrease relatively slowly, indicating that several dozen occupied-virtual geminals on each monomer are needed for a reasonable description of the amplitudes. By contrast, the singular values associated with $\mathcal{T}_2^{disp}$ exhibit a very sharp decrease already at 3.0 Å, the shortest distance explored in this work. Increasing the basis set angular momentum or adding diffuse functions does not affect significantly the initial decrease for the 3.0 Å distance, but a longer tail appears for singular values comprised between 10^{-5} and 10^{-8}. As the interatomic distance increases, singular values decay more and more sharply. In addition, when exchange effects become negligible at 6.0 Å and beyond, increasing the basis set angular momentum or diffuse character has very little effect on the total number of singular values larger than 10^{-8}. For the following computations, and unless mentioned otherwise, we thus choose the d-aug-cc-pVQZ basis set. We validated the robustness of the He_2 trend on other small dispersion-dominated dimers: He interacting with a monomer containing more than one electron pair (He$\cdots$Be) or more than one atom (He$\cdots H_2$) and two hydrogen atoms at the triplet and singlet states, prototypes of same-spin and opposite-spin dispersion, respectively (see Fig. S1 of the supplementary material). All cases are consistent with our observations on He_2.

In Fig. 2, we plotted in more detail the first few $\mathcal{T}_2^{disp}$ singular values, which are associated with the most important geminals for each dimer. Most systems at all distances exhibit a group of three singular values that are more significant than the others and dominate the description of dispersion interactions. This feature becomes more obvious at 6.0 Å and larger distances, as exchange effects become negligible. The only exception is H_2 singlet at 3.0 Å where the orbitals tend to be more delocalized, possibly because of the absence of Pauli repulsion and the emerging covalent bond, which blurs our definition of dispersion.

In all systems at 9.0 Å, we distinguish a further group of 8 singular values before another discontinuity. In the case of He_2, this group of 8 shows an emerging internal structure that divides it in 3 values followed by 5. The origin of this division will become clearer as we examine the composition of the virtual space for each geminal in Sec. III B. We further remark that the contrast between the intraatomic and dispersion-related singular values is even more striking at this scale.

In the smaller basis sets cc-pVTZ, cc-pVQZ, aug-cc-pVTZ, and aug-cc-pVQZ for He_2, we observe the same structure for the first few singular values (see Fig. S2 of the supplementary material), which confirms the robustness of this trend. As the basis set becomes larger and more diffuse, the 3 first singular values are still clearly separated from the rest, although the following structure becomes less visible.

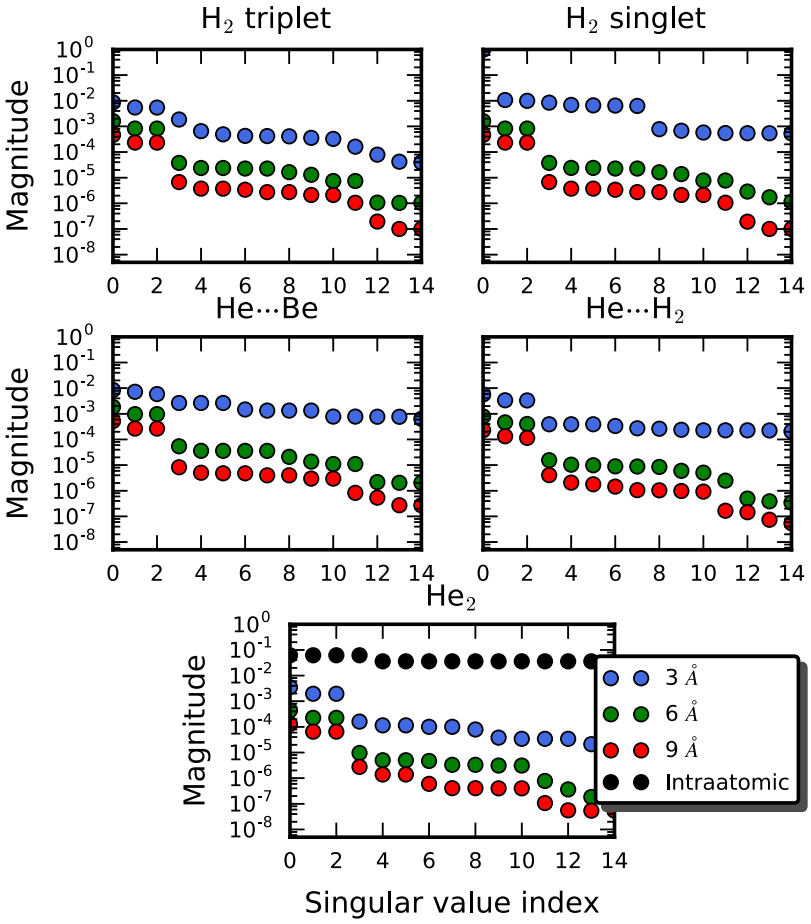

FIG. 2. 15 first singular values of $\mathcal{T}_2^{disp}$ for H_2 triplet and singlet, He$\cdots$Be, He$\cdots H_2$, and He_2 with the d-aug-cc-pVQZ basis set at 3.0 (blue), 6.0 (green), and 9.0 Å (red) monomer separation. For He_2, singular values for the intraatomic amplitude tensor $\mathcal{T}_2^{intra}$ are also shown in black. The computed dimer is identified above each plot.

B. Virtual components of geminals

As detailed in Sec. II B, each singular vector from the SVD of $\mathcal{T}_2^{disp}$ is a geminal with $O_X V_X$ elements, having components in both the occupied and virtual spaces. To examine the virtual orbitals, we unfold each geminal in a matrix with O_X rows and V_X columns that is decomposed by SVD in pairs of occupied and virtual orbitals (similarly to a NTO[50] analysis) completely representing the original matrix. In the small monomers studied here, there is only one occupied orbital and thus only one virtual orbital per geminal.

We plot these virtual orbitals for the 11 most important geminals in Fig. 3 at 6.0 Å interatomic separation for He_2. The data at 3.0 and 9.0 Å are presented in Figs. S3 and S4 of the supplementary material and demonstrate that results are converged in practice at 6.0 Å. At all distances, the virtual part of the three first geminals corresponds to three 2p orbitals, one per geminal (see Fig. 3 and Fig. S3 of the supplementary material, geminals 1-3). We can interpret each geminal as describing an excitation from an occupied 1s to a virtual 2p orbital. Hence, the three first geminals correspond to the pure dipole-dipole interactions in Eq. (9), which we expect to decay as R^{-6} and to dominate dispersion interactions at long range.[39]

The three next geminals at 6.0 Å and beyond clearly resemble 3p orbitals (see geminals 4-6 in Fig. 3), with geminals 5 and 6 showing signs of polarization. The physical role of 3p orbitals appears less clear but could be connected to the next non-zero term in the multipolar expansion of dispersion for atoms,[39] the mixed dipolar-quadrupolar interactions [see Eq. (9)]. Geminals 7-11 display a clear 3d character at long range (see Fig. 3). Physically, we attribute these orbitals to the next non-zero term for atoms in the multipolar expansion of dispersion which contains pure quadrupole-quadrupole interactions. At 3.0 Å separation, exchange and overlap effects modify the shape of geminals 4-11 virtual orbitals. Geminals 4-8 virtuals resemble mixtures of 3d and 3p orbitals, while geminals 9-11 are not easily recognizable. However, virtuals corresponding to geminals 1-3 are always identifiable as 2p orbitals (see Figs. S3 and S4 of the supplementary material).

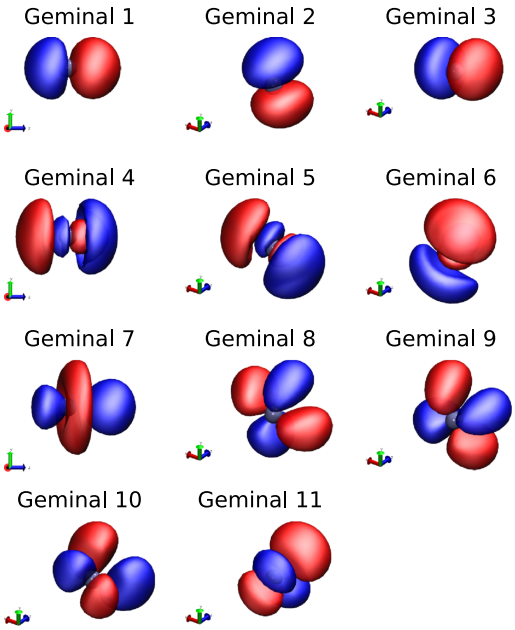

FIG. 3. Virtual part of geminals 1 to 11 (left to right, top to bottom) for He_2 with the d-aug-cc-pVQZ basis at 6.0 Å interatomic separation. Orbitals are plotted at an isovalue of 0.05. The interacting partner is located along the z axis, represented in blue.

For all groups of similar geminals, the one aligned with the interatomic axis is generally associated with a slightly larger singular value and thus describes a larger portion of $\mathcal{T}_2^{disp}$. The shape and the ordering of the virtual orbitals depicted above seem to be typical of two-electron systems, as shown by computations on other small monomers (see Figs. S5–S12 of the supplementary material). Even the diatomic H_2 asymptotically displays geminal virtuals reminiscent of 2p, 3p, and 3d orbitals when interacting with He.

Finally, we can now explain the structure of the singular values observed in Sec. III A. The dominant three singular values are associated with the three 2p orbitals that correspond to dominant dipole-dipole interactions. The next group of 8 singular values gathers three 3p and five 3d orbitals, from where the substructure of three and five singular values that we noticed for some systems originates.

C. Distance dependence of singular values

As the interatomic distance increases, we expect the dispersion energy to decrease asymptotically as R^{-6}. Equation (1) shows that the dispersion energy results from the contraction of integrals and amplitudes. To second order, the amplitudes are computed directly from the MO integrals and energies as shown in Eq. (2). We can thus expect the decay rate of the amplitudes (and thus of the corresponding singular values) to be roughly the square root of the decay rate for the energy. We fitted the singular values for He_2/d-aug-cc-pVQZ with a $f(x) = b \cdot x^A$ function where $f(x)$ is the singular value, x is the interatomic distance, and A and b are the fitted parameters. We report the decay exponents A obtained in Table I.

The three first singular values decay approximately as R^{-3}, the three next as R^{-4}, and the 5 last as R^{-5}. Note that the decay exponents are a bit less accurate for this last group because of their very low magnitude at large distances. Thus, the decay behavior associated with the 2p-like virtuals corresponds to a decay of the energy as R^{-6} consistent with dipole-dipole interactions. The energy associated with the 3p-like virtuals decays approximately as R^{-8}, which corresponds to the expected decay for dipole-quadrupole interactions. Finally, the energy associated with the 3d orbitals behaves as R^{-10}, confirming its relation to quadrupole-quadrupole interactions. Note that terms decaying as odd powers of R vanish for atoms and centrosymmetric molecules. Thus our interpretation of the physical role of the different virtual orbitals and the decay

TABLE I. Exponents A for the fitting curves $f(x) = b \cdot x^A$ where $f(x)$ is a singular value and x is the interfragment distance for He_2/d-aug-cc-pVQZ.

Singular value index	0	1	2	3	4	5
Exponent A	−2.90	−3.07	−3.06	−3.98	−4.40	−4.40
Singular value index	6	7	8	9	10	
Exponent A	−5.02	−5.16	−5.01	−4.77	−4.56	

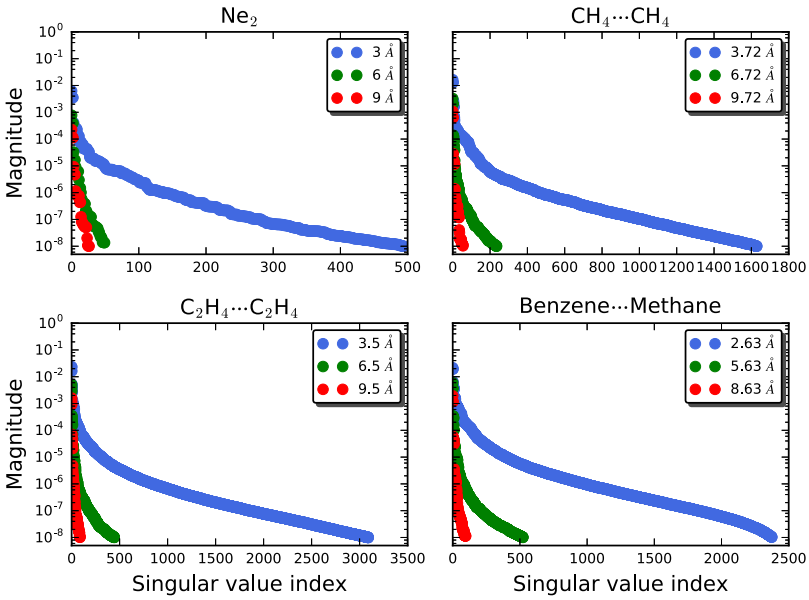

FIG. 4. $\mathcal{T}_2^{disp}$ singular values for Ne_2, methane dimer, ethene dimer, and methane-benzene dimer at various interfragment distances as indicated on each plot. Ne_2 was computed with aug-cc-pVQZ and all other systems were computed with aug-cc-pVTZ.

behavior of the associated amplitudes are consistent with the multipolar expansion of dispersion shown in Eq. (9).[39]

D. Polyatomic monomers

Turning to systems with multiple electron pairs, we plot the singular values obtained from the SVD of $\mathcal{T}_2^{disp}$ for Ne_2, methane dimer, ethene dimer, and methane-benzene dimer in Fig. 4. In all these cases, the singular values decay extremely quickly, and their decay becomes even more pronounced as the interfragment distance increases. It is remarkable that even in these larger systems, only a very small number of geminals, i.e., excitations, are necessary for a compact description of the $\mathcal{T}_2^{disp}$ tensor. A closer look at the singular values (see Fig. S13 of the supplementary material) reveals the same structure than for small monomers: a group of 3 singular values clearly dominates the description of $\mathcal{T}_2^{disp}$ at all distances, likely associated with dipole-dipole interactions. Even the secondary structure of 8 singular values is visible, with a subdivision in a group of 3 and a group of 5 that is only distinguishable at longer distances in some systems, corresponding to the dipole-quadrupole and quadrupole-quadrupole terms. Thus, our observations regarding the decay behavior and the structure of the $\mathcal{T}_2^{disp}$ singular values are robust with respect to a monomer size.

IV. APPROXIMATE DISPERSION ENERGIES

Our analysis up to now has been confined to the amplitude tensor $\mathcal{T}_2^{disp}$. However, the dispersion energy is computed by contracting $\mathcal{T}_2^{disp}$ with appropriate two-electron integrals over molecular orbitals. Does our analysis carry over from amplitudes to dispersion energies? To investigate this question, we reconstruct $\mathcal{T}_2^{disp}$ approximately from Eq. (10) by including only the N_{gem} most important geminals as columns of the matrices $\mathbf{G}^A$ and $\mathbf{G}^B$. We then compute the dispersion energy with the approximated $\mathcal{T}_2^{disp}$, which corresponds to computing dispersion energies in a restricted virtual space containing only the virtual orbitals extracted from the N_{gem} most important geminals that we plotted in Sec. III B. We then assess the accuracy of this approximate representation by comparing it with the dispersion energy obtained from the exact $\mathcal{T}_2^{disp}$.

A. Small monomers

We probed the accuracy of approximate dispersion energies in the 5 small monomers studied previously and plotted the results at 3.0, 6.0, and 9.0 Å for various values of N_{gem} in Fig. 5. We immediately see that the results are good, with errors below 0.5% at distances larger than 3.0 Å for all N_{gem} tested. Using only $N_{gem} = 3$, the error converges asymptotically to a small but constant value inferior to 0.3% of the full dispersion energy at long distances (≥6.0 Å). For further improvement, we add the next set of virtual orbitals corresponding to 3p-like functions. In this case, $N_{gem} = 6$ in total and the relative errors asymptotically converge to zero.

At the shortest distance of 3.0 Å, He···Be and ground state H_2 at the singlet state exhibit larger errors. These are caused by the larger size of Be which increases the importance of the exchange terms and by traces of covalent character in singlet H_2. Even in these two cases, the error decreases rapidly with distance to a small constant for 3 geminals and to practically zero for 6 geminals and more. We found consistent trends for He_2 at various distances and with different basis sets (see Fig. S14 of the supplementary material).

In all the small systems, we can thus describe dispersion energies with at least 99.5% accuracy at 6.0 Å and beyond using only three geminals per atom to represent the dispersion amplitudes. At short distances, exchange effects make our definition of dispersion unreliable, but 6 geminals per atom still generally describe 90% of electron correlation.

B. Polyatomic monomers

Since the singular values of $\mathcal{T}_2^{disp}$ behave in a similar way between the small and large monomers, we expect that an

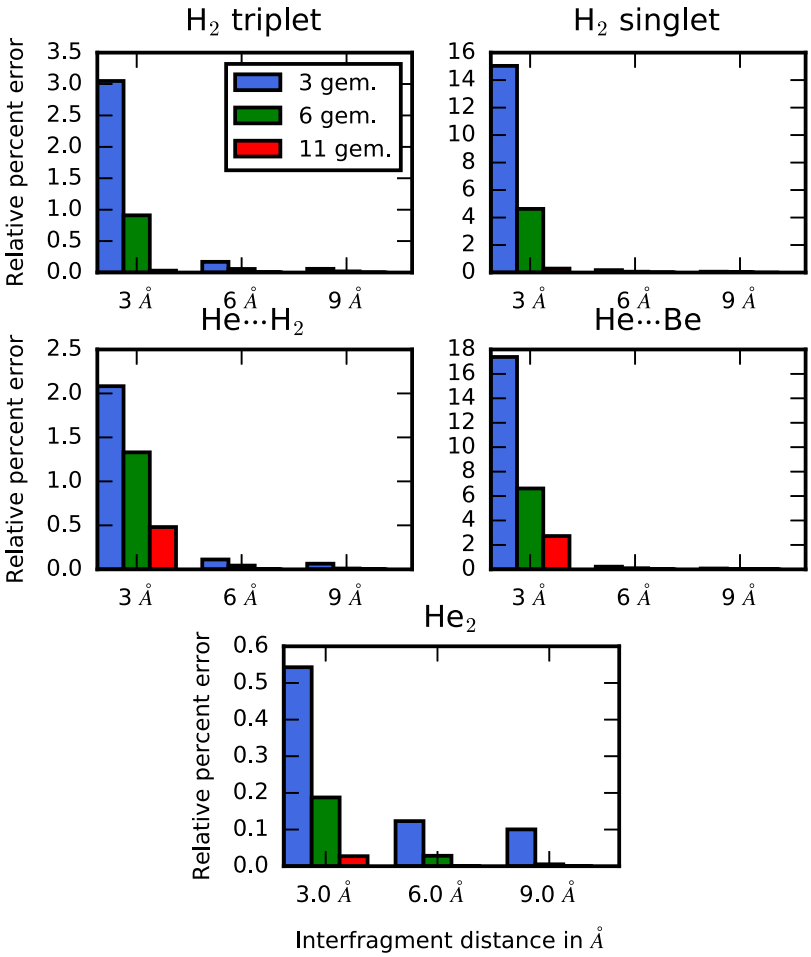

FIG. 5. Relative percent error for dispersion energy computed with $\mathcal{T}_2^{disp}$ approximately reconstructed with 3 (blue), 6 (green), and 11 (red) geminals at 3.0, 6.0, and 9.0 Å for H_2 triplet, H_2 singlet, He$\cdots$H$_2$, He$\cdots$Be, and He_2 with the d-aug-cc-pVQZ basis set. Each system is indicated above the corresponding plot.

accurate and compact description of dispersion energies is possible for polyatomic systems using only 3 geminals.

In Fig. 6, we plot relative errors obtained for 3, 6, 8, 11, and 15 geminals for Ne_2, methane dimer, ethene dimer, and methane-benzene dimer. Indeed, 3 geminals provide an excellent description of dispersion interactions. Even at the shortest distance, we recover between 85% and 99% of the CCSD dispersion energy. As the interfragment distance increases, the relative error decreases to a constant value below 0.5%. Adding 3 more geminals to the description of dispersion so that $N_{gem} = 6$ reduces the error at all distances and makes the long-range error negligible. At all distances, increasing N_{gem} further decreases the error until we obtain numerically exact results. Hence, all of the essential observations that were made on small monomers carry over to larger molecules, and we can be quite confident that these trends are general.

Since we localize orbitals to identify dispersion in the CCSD energy, we assessed the relative importance of σ and π electrons in dispersion interactions in the ethene dimer and the ethene-ethyne dimer. We find that although the individual contributions of π electrons are larger than those of σ electrons, there is usually many more σ than π electrons and both contribute significantly. This is in agreement with other literature findings.[60–62] We also verified that the relative contribution of σ and π electrons was well-represented by our approximate $\mathcal{T}_2^{disp}$ (see the supplementary material for a more detailed discussion).

C. Properties of the virtual space

As mentioned before, each geminal can be decomposed into O_X pairs of occupied and virtual orbitals that completely describe it. Thus, there are in general N_{occ} virtual orbitals per geminal, which means that the necessary N_{gem} geminals to describe dispersion accurately in a given dimer correspond to the number of virtual orbitals needed *per occupied orbital*.

We emphasize that virtual orbitals obtained from different geminals are not orthogonal and in fact may not even be linearly independent in the general case. We examined the rank of the virtual space obtained by the union of the virtual orbitals from the 3 first and then from the 6 first geminals. For this purpose, we build the overlap matrix of the virtual orbitals investigated and examine its eigenvalues. Except for Ne_2, all overlap matrices are full rank which indicates that all of the $3N_{occ}$ or $6N_{occ}$ virtuals are necessary to describe the space spanned by 3 and 6 geminals, respectively. For Ne_2, there is one linearly dependent virtual for $N_{gem} = 3$ at all distances, whereas for $N_{gem} = 6$ there is one linearly dependent virtual at the shortest distance and two at 6.0 and 9.0 Å. We attribute this small redundancy of the virtual space to the high symmetry of the dimer. One of these virtual orbitals however is paired with a core occupied orbital. We can discard all such orbital pairs by performing a frozen core computation, introducing only a minor error ranging from 0.05% to 0.2% compared to

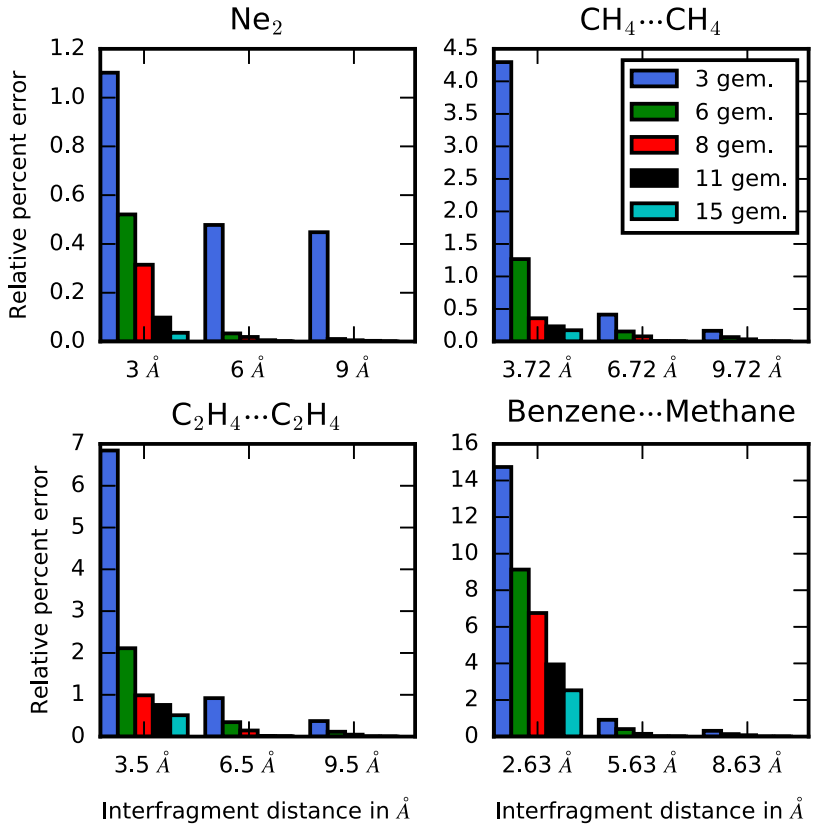

FIG. 6. Relative percent error for dispersion energy computed with $\mathcal{T}_2^{disp}$ approximately reconstructed with 3 (blue), 6 (green), 8 (red), 11 (black), and 15 (teal) geminals at various distances for Ne_2, methane dimer, ethene dimer, and benzene-methane dimer. Ne_2 was computed with aug-cc-pVQZ and all other systems were computed with aug-cc-pVTZ.

the full electron computation (see Table SII and discussion in the supplementary material).

Examining again Eq. (11) that connects the unfolded tensor of dispersion amplitudes to the geminals

$$\mathbf{T}^{O_A V_A, O_B V_B} = \sum_{P}^{N_{gem}} \mathbf{G}^{A}_{\bullet P} \gamma_P \left(\mathbf{G}^{B}_{\bullet P}\right)^T, \tag{13}$$

we see that each geminal on monomer A is only coupled to one geminal on monomer B. Hence, with 3 geminals per monomer, the above sum has only 3 terms. In addition, the singular values γ_P directly represent dispersion amplitudes t_{ij}^{ab} transformed to the geminal basis. Thus, there exists in principle a transformation of the amplitudes that allows us to describe dispersion interactions with only 3 to 6 non-zero transformed amplitudes for a dimer. In principle this provides an extremely efficient description of dispersion; however, optimizing coupled-cluster amplitudes in such a geminal basis is far from trivial. In addition, the geminal transformation would have to be obtained *a priori* with sufficient accuracy.

A simpler alternative for an efficient description of dispersion is to find an appropriate reduced virtual orbital basis. In PNO-type methods, such a basis is extracted from approximate MP2 amplitudes for each local occupied orbital pair, and we could envision a similar strategy. Recently, Werner specifically investigated distant pairs[38] and found that 3 to 4 distant PNOs (dPNOs) were associated with each occupied orbital. As we mentioned in Sec. II B, our two-step SVD decomposition applied to a single orbital pair yields PNOs. Since we also considered long-range correlation, our analysis of small monomers (one occupied pair) yields dPNOs from CCSD amplitudes and we directly confirm Werner's results: 3 dPNOs yield accurate dispersion energies. However, our method is not restricted to a single occupied pair and our results on polyatomic molecules show that, in general, only 3 to 6 (O_A + O_B) virtuals are necessary for dispersion. dPNOs are computed for each orbital pair, yielding $3O_AO_B$ virtuals. Thus, our results indicate redundancy in the dPNO space and a possibility to further reduce the virtual space needed to describe dispersion, at the expense of a two-step SVD on the amplitude tensor. Whether or not such a reduction would be advantageous will obviously depend on the relative costs of the dispersion computation with respect to the SVD.

Furthermore, our results give us access to the shape of dispersion-optimized virtual orbitals for various systems, hence we can explore a wider variety of ideas to obtain an efficient virtual basis for dispersion. As an example, since our decomposition of geminals is similar to the NTO analysis, we examine the adequacy of NTO orbitals to describe dispersion. A simple CIS computation on atomic He shows us that the orbitals do not appear in the desired order: 3p NTOs come after 3s and 3d orbitals, instead of being directly after 2p. In addition, an overlay of NTOs with dispersion-optimal virtuals clearly indicates that NTOs are generally too diffuse (see Fig. S15 of the supplementary material). Thus, NTOs are unlikely to yield an accurate description of the electronic excitations giving rise to dispersion. This is in agreement with the slow convergence of the sum-over-state expression for dispersion, indicating that excited states are not an optimal basis to describe this phenomenon. Investigations are currently underway in our laboratory to determine other ways of obtaining virtuals well-tailored to describe dispersion interactions.

V. CONCLUSIONS

We have investigated compressed representations of the dispersion amplitude tensor $\mathcal{T}_2^{disp}$ from CCSD computations using large basis sets on He_2, H_2 singlet and triplet, $He\cdots Be$, and $He\cdots H_2$ at different separations. Grouping indices from the same monomer together, $\mathcal{T}_2^{disp}$ is written as a matrix that we can decompose by SVD in monomer geminal vectors, each describing an excitation process. In all cases, even at relatively short distances, the associated singular values display a sharp decrease, indicating that only a few geminals are needed to represent $\mathcal{T}_2^{disp}$. Closer examination indicated that a group of 3 singular values dominated the others, followed by another group of 8 singular values. For small monomers, further SVD of each geminal vector yields one dominant virtual-occupied orbital pair. For the three most important geminals, we obtain three virtual 2p orbitals. The next group of 8 geminals is composed of 3p-like orbitals, dominating at long range over five 3d-like orbitals. We connected the observed orbital shapes to the multipolar expansion of dispersion energies by examination of the decay behavior of the corresponding singular values. In atoms with a 1s occupied orbital, 2p virtual orbitals are describing dipole-dipole correlations, 3p orbitals are probably linked to dipole-quadrupole interactions, and 3d orbitals to quadrupole-quadrupole interactions. We verified that our analysis carried over to polyatomic monomers by examining singular values for Ne_2, methane dimer, ethene dimer, and methane-benzene dimer.

Using only 3 geminals on each monomer, we reconstructed the original $\mathcal{T}_2^{disp}$ to a very good accuracy. This accuracy is transferable to the dispersion energies themselves with small relative errors obtained at all distances. At long distances, a reconstruction based on 3 geminals yields a small constant relative error, which disappears on including 3 additional geminals. This result is also valid for larger, polyatomic systems, demonstrating that efficient compressed representations for long-range dispersion energies exist.

The virtual space connected to such a representation is composed of a small number of low angular momentum functions, which in general must only be able to describe a dipolar electronic excitation from each occupied orbital. There are no more than 3 of these per occupied orbital (just as the linear response of the SCF wavefunction to a uniform field requires only 3 virtuals per occupied[63]). This directly fulfills Pulay's prediction,[29] already mentioned in the Introduction, as well as similar hints in the symmetry-adapted perturbation theory literature.[64] It also explains the success of explicitly correlated methods[65] for non-covalent interactions since the low angular momentum basis sets used are sufficient to describe long-range dispersion while the short-range electron correlation is taken care of by the explicit correlation technique.

Our results open new ways to approximate dispersion interactions efficiently. In principle, coupled-cluster amplitudes can be transformed to accurately describe long-range dispersion using as few as 3 geminals. Finding the appropriate transformation and amplitude optimization method is however challenging. Another possibility, exploited by Werner in his recent work on dPNOs,[38] is to define a reduced virtual space specifically tailored for dispersion on each monomer. Work is currently underway in our laboratory to find even simpler alternatives yielding dispersion-optimized virtuals. Such approaches may be useful for defining the dispersion contribution in energy decomposition analysis methods based on wavefunction methods.[43,66,67] Finally, we hinted at the importance of dipole-quadrupole terms to accelerate the long-range convergence of dispersion energies, which could be useful in numerous approximate dispersion methods.

SUPPLEMENTARY MATERIAL

See supplementary material for a discussion of the relative contribution of σ and π electrons to dispersion and of frozen core approximation errors; additional figures for singular values, dispersion energies, and virtual orbitals for all systems studied; and tables of dispersion energies and the corresponding relative errors for all systems.

ACKNOWLEDGMENTS

The authors acknowledge the anonymous reviewers for their comments, which helped improve this manuscript. This work was supported by grants from the U.S. National Science Foundation (Nos. CHE-1363342 and CHE-1665315). J.F.G. acknowledges Grant No. P300P2_164631 from the Swiss National Science Foundation.

[1] T. Helgaker, P. Jorgensen, and J. Olsen, *Molecular Electronic-Structure Theory* (John Wiley & Sons, Ltd., 2000).
[2] G. Golub and C. Van Loan, *Matrix Computations*, 4th ed. (Johns Hopkins, Baltimore, 2013).
[3] J. L. Whitten, J. Chem. Phys. **58**, 4496 (1973).
[4] B. I. Dunlap, J. W. D. Connolly, and J. R. Sabin, J. Chem. Phys. **71**, 3396 (1979).
[5] B. I. Dunlap, Phys. Chem. Chem. Phys. **2**, 2113 (2000).
[6] O. Vahtras, J. Almlof, and M. Feyereisen, Chem. Phys. Lett. **213**, 514 (1993).
[7] M. Feyereisen, G. Fitzgerald, and A. Komornicki, Chem. Phys. Lett. **208**, 359 (1993).
[8] H. Koch, A. Sanchez de Meras, and T. B. Pedersen, J. Chem. Phys. **118**, 9481 (2003).
[9] I. Roeggen and E. Wisloff-Nilssen, Chem. Phys. Lett. **132**, 154 (1986).
[10] N. H. F. Beebe and J. Linderberg, Int. J. Quantum Chem. **12**, 683 (1977).
[11] T. Kinoshita, O. Hino, and R. J. Bartlett, J. Chem. Phys. **119**, 7756 (2003).
[12] O. Hino, T. Kinoshita, and R. J. Bartlett, J. Chem. Phys. **121**, 1206 (2004).
[13] G. J. O. Beran and M. Head-Gordon, J. Chem. Phys. **121**, 78 (2004).
[14] L. D. Lathauwer, B. D. Moor, and J. Vandewalle, SIAM J. Matrix Anal. Appl. **21**, 1253 (2000).
[15] F. Bell, D. Lambrecht, and M. Head-Gordon, Mol. Phys. **108**, 2759 (2010).
[16] U. Benedikt, H. Auer, M. Espig, W. Hackbusch, and A. A. Auer, Mol. Phys. **111**, 2398 (2013).
[17] U. Benedikt, K.-H. Bohm, and A. A. Auer, J. Chem. Phys. **139**, 224101 (2013).
[18] C. A. Schwerdtfeger and D. A. Mazziotti, J. Chem. Phys. **137**, 244103 (2012).
[19] E. G. Hohenstein, R. M. Parrish, and T. J. Martinez, J. Chem. Phys. **137**, 044103 (2012).
[20] R. M. Parrish, E. G. Hohenstein, T. J. Martinez, and C. D. Sherrill, J. Chem. Phys. **138**, 194107 (2013).
[21] E. P. Hoy and D. A. Mazziotti, J. Chem. Phys. **143**, 064103 (2015).
[22] S. R. White and R. M. Noack, Phys. Rev. Lett. **68**, 3487 (1992).
[23] S. R. White, Phys. Rev. Lett. **69**, 2863 (1992).
[24] G. K.-L. Chan and D. Zgid, in *Annual Reports in Computational Chemistry*, edited by R. A. Wheeler (Elsevier, 2009), Vol. 5, pp. 149–162.
[25] P.-O. Löwdin and H. Shull, Phys. Rev. **101**, 1730 (1956).
[26] T. L. Barr and E. R. Davidson, Phys. Rev. A **1**, 644 (1970).
[27] W. Klopper, J. Noga, H. Koch, and T. Helgaker, Theor. Chem. Acc. **97**, 164 (1997).

[28]A. G. Taube and R. J. Bartlett, Collect. Czech. Chem. Commun. **70**, 837 (2005).
[29]P. Pulay, Chem. Phys. Lett. **100**, 151 (1983).
[30]S. Saebo and P. Pulay, Annu. Rev. Phys. Chem. **44**, 213 (1993).
[31]C. Edmiston and M. Krauss, J. Chem. Phys. **42**, 1119 (1965).
[32]C. Edmiston and M. Krauss, J. Chem. Phys. **45**, 1833 (1966).
[33]F. Neese, F. Wennmohs, and A. Hansen, J. Chem. Phys. **130**, 114108 (2009).
[34]C. Riplinger and F. Neese, J. Chem. Phys. **138**, 034106 (2013).
[35]J. Yang, Y. Kurashige, F. R. Manby, and G. K. L. Chan, J. Chem. Phys. **134**, 044123 (2011).
[36]M. Schutz, J. Yang, G. K.-L. Chan, F. R. Manby, and H.-J. Werner, J. Chem. Phys. **138**, 054109 (2013).
[37]J. Yang, G. K.-L. Chan, F. R. Manby, M. Schutz, and H.-J. Werner, J. Chem. Phys. **136**, 144105 (2012).
[38]H.-J. Werner, J. Chem. Phys. **145**, 201101 (2016).
[39]A. J. Stone, *The Theory of Intermolecular Forces* (Oxford University Press, Oxford, 1996).
[40]P. Jurecka, J. Sponer, J. Cerny, and P. Hobza, Phys. Chem. Chem. Phys. **8**, 1985 (2006).
[41]S. M. Cybulski and M. L. Lytle, J. Chem. Phys. **127**, 141102 (2007).
[42]M. Schutz, G. Rauhut, and H.-J. Werner, J. Phys. Chem. A **102**, 5997 (1998).
[43]R. J. Azar and M. Head-Gordon, J. Chem. Phys. **136**, 024103 (2012).
[44]W. B. Schneider, G. Bistoni, M. Sparta, M. Saitow, C. Riplinger, A. A. Auer, and F. Neese, J. Chem. Theory Comput. **12**, 4778 (2016).
[45]S. Boys, in *Quantum Science of Atoms, Molecules, and Solids*, edited by P. Löwdin (Academic Press, New York, 1966), p. 253.
[46]S. F. Boys, Rev. Mod. Phys. **32**, 296 (1960).
[47]J. E. Subotnik, Y. Shao, W. Liang, and M. Head-Gordon, J. Chem. Phys. **121**, 9220 (2004).
[48]J. E. Subotnik, A. Sodt, and M. Head-Gordon, Phys. Chem. Chem. Phys. **9**, 5522 (2007).
[49]N. Vannieuwenhoven, R. Vandebril, and K. Meerbergen, SIAM J. Sci. Comput. **34**, A1027 (2012).
[50]A. V. Luzanov, A. A. Sukhorukov, and V. É. Umanskii, Theor. Exp. Chem. **10**, 354 (1976).
[51]R. L. Martin, J. Chem. Phys. **118**, 4775 (2003).
[52]I. Mayer, Chem. Phys. Lett. **437**, 284 (2007).
[53]W. Humphrey, A. Dalke, and K. Schulten, J. Mol. Graphics **14**, 33 (1996).
[54]D. E. Woon and T. H. Dunning, J. Chem. Phys. **100**, 2975 (1994).
[55]R. A. Kendall, T. H. Dunning, and R. J. Harrison, J. Chem. Phys. **96**, 6796 (1992).
[56]T. H. Dunning, Jr., J. Chem. Phys. **90**, 1007 (1989).
[57]J. Rezac and P. Hobza, J. Chem. Theory Comput. **9**, 2151 (2013).
[58]J. Rezac, P. Jurecka, K. E. Riley, J. Cerny, H. Valdes, K. Pluhackova, K. Berka, T. Rezac, M. Pitonak, J. Vondrasek, and P. Hobza, Collect. Czech. Chem. Commun. **73**, 1261 (2008).
[59]Y. Shao, Z. Gan, E. Epifanovsky, A. T. Gilbert, M. Wormit, J. Kussmann, A. W. Lange, A. Behn, J. Deng, X. Feng, D. Ghosh, M. Goldey, P. R. Horn, L. D. Jacobson, I. Kaliman, R. Z. Khaliullin, T. Kus, A. Landau, J. Liu, E. I. Proynov, Y. M. Rhee, R. M. Richard, M. A. Rohrdanz, R. P. Steele, E. J. Sundstrom, H. L. Woodcock III, P. M. Zimmerman, D. Zuev, B. Albrecht, E. Alguire, B. Austin, G. J. O. Beran, Y. A. Bernard, E. Berquist, K. Brandhorst, K. B. Bravaya, S. T. Brown, D. Casanova, C.-M. Chang, Y. Chen, S. H. Chien, K. D. Closser, D. L. Crittenden, M. Diedenhofen, R. A. DiStasio, Jr., H. Do, A. D. Dutoi, R. G. Edgar, S. Fatehi, L. Fusti-Molnar, A. Ghysels, A. Golubeva-Zadorozhnaya, J. Gomes, M. W. Hanson-Heine, P. H. Harbach, A. W. Hauser, E. G. Hohenstein, Z. C. Holden, T.-C. Jagau, H. Ji, B. Kaduk, K. Khistyaev, J. Kim, J. Kim, R. A. King, P. Klunzinger, D. Kosenkov, T. Kowalczyk, C. M. Krauter, K. U. Lao, A. D. Laurent, K. V. Lawler, S. V. Levchenko, C. Y. Lin, F. Liu, E. Livshits, R. C. Lochan, A. Luenser, P. Manohar, S. F. Manzer, S.-P. Mao, N. Mardirossian, A. V. Marenich, S. A. Maurer, N. J. Mayhall, E. Neuscamman, C. M. Oana, R. Olivares-Amaya, D. P. O'Neill, J. A. Parkhill, T. M. Perrine, R. Peverati, A. Prociuk, D. R. Rehn, E. Rosta, N. J. Russ, S. M. Sharada, S. Sharma, D. W. Small, A. Sodt, T. Stein, D. Stuck, Y.-C. Su, A. J. Thom, T. Tsuchimochi, V. Vanovschi, L. Vogt, O. Vydrov, T. Wang, M. A. Watson, J. Wenzel, A. White, C. F. Williams, J. Yang, S. Yeganeh, S. R. Yost, Z.-Q. You, I. Y. Zhang, X. Zhang, Y. Zhao, B. R. Brooks, G. K. Chan, D. M. Chipman, C. J. Cramer, W. A. Goddard III, M. S. Gordon, W. J. Hehre, A. Klamt, H. F. Schaefer III, M. W. Schmidt, C. D. Sherrill, D. G. Truhlar, A. Warshel, X. Xu, A. Aspuru-Guzik, R. Baer, A. T. Bell, N. A. Besley, J.-D. Chai, A. Dreuw, B. D. Dunietz, T. R. Furlani, S. R. Gwaltney, C.-P. Hsu, Y. Jung, J. Kong, D. S. Lambrecht, W. Liang, C. Ochsenfeld, V. A. Rassolov, L. V. Slipchenko, J. E. Subotnik, T. V. Voorhis, J. M. Herbert, A. I. Krylov, P. M. Gill, and M. Head-Gordon, Mol. Phys. **113**, 184 (2015).
[60]M. Alonso, T. Woller, F. J. Martin-Martinez, J. Contreras-Garcia, P. Geerlings, and F. De Proft, Chem. - Eur. J. **20**, 4931 (2014).
[61]T. Janowski and P. Pulay, J. Am. Chem. Soc. **134**, 17520 (2012).
[62]A. A. Fokin, D. Gerbig, and P. R. Schreiner, J. Am. Chem. Soc. **133**, 20036 (2011).
[63]P. R. Horn and M. Head-Gordon, J. Chem. Phys. **143**, 114111 (2015).
[64]A. J. Misquitta and K. Szalewicz, J. Chem. Phys. **122**, 214109 (2005).
[65]D. A. Sirianni, L. A. Burns, and C. D. Sherrill, J. Chem. Theory Comput. **13**, 86 (2017).
[66]J. Thirman and M. Head-Gordon, J. Chem. Phys. **143**, 084124 (2015).
[67]J. Thirman and M. Head-Gordon, J. Phys. Chem. A **121**, 717 (2017).